JOURNAL OF MATERIALS SCIENCE 31 (1996) 3053–3056

Solid-state kinetics and reaction mechanisms for the formation of $Y_2Cu_2O_5$

N. AKHTAR, R. JANES, M. J. PARKER
Department of Chemistry, Manchester Metropolitan University, John Dalton Building, Chester Street, Manchester M1 5GD, UK

The kinetics of $Y_2Cu_2O_5$ formation by the solid-state reaction between Y_2O_3 and CuO were followed by quantitative X-ray powder diffraction, the initial nucleation stages being probed by EPR spectroscopy. Analysis of fractional reaction versus time data showed a best fit to the mathematical model of Jander, with an activation energy of 58.2 kcal mol^{-1}. Preliminary comparative studies, employing different preparative routes; coprecipitation, accelerants and combustion synthesis are also reported.

1. Introduction

The kinetics and mechanism of formation of cuprate superconductors e.g. $YBa_2Cu_3O_7$ are not as yet fully discussed in the literature. The solid-state reaction between Y_2O_3, CuO and $BaCO_3$ would appear most complex, and traditional techniques such as thermogravimetry and differential thermal analysis do not allow complete mechanistic elucidation. During synthesis of polycrystalline superconducting $Bi_2Sr_2CuO_x$, Ghinga *et al.* [1] have established a clear correlation between kinetic factors and product composition during standard solid-state synthesis. The rate of product formation in additive solid–solid reactions may be governed by diffusion of reactants through a continuous product layer, nucleation of the product at active sites and growth of nucleated particles, or reactions at phase interfaces. Mechanisms such as those of Jander [2], Ginstling and Brounstein [3] and others [4] have been proposed for solid-state reaction, each of which varies in the initial assumptions used in their derivation.

Extensive experimental evidence has led to the widespread belief that solid-state reactions are initiated at nucleation sites, followed by growth of a reactant product interface which advances into the unreacted precursor [5]. Commonly, kinetic data from solid-state reaction is expressed in terms of the fractional reaction completed (α) as a function of time in an isothermal reaction [5] i.e. $\alpha = f(kt)$ where k is the kinetic rate constant. Typically, fitting isothermal data to established rate equations derived from geometric considerations is an accepted means of establishing the applicability of a particular model. Ultimately, we would expect to comment on the mechanism of reaction.

In this work, a common parasitic phase frequently observed during synthesis of $YBa_2Cu_3O_7$, namely $Y_2Cu_2O_5$ (often referred to as "blue phase"), is chosen as a starting point with which to initiate a study of reaction kinetics within this system. The binary, semiconducting $Y_2Cu_2O_5$, is readily formed by reaction of Y_2O_3 and CuO [6], and has been extensively investigated from a magnetic viewpoint, exhibiting both ferromagnetic and antiferromagnetic interactions [7, 8, 9]. Structurally, Cu^{2+} ions are linked by Cu–O–Cu bridges with 90° bond angles forming chains of Cu_2O_8 dimeric units. It is proposed that ferromagnetic ordering exists within the chains, which order antiferromagnetically at low temperatures (ca. 13 K). The manipulation of the magnetic properties of this phase by chemical substitution, has recently been reported by Su and coworkers [10].

In general, we would expect kinetics and mechanism to be inextricably linked to the type of synthetic route employed. Preparation of high-T_c superconductors and related cuprate insulators, is most commonly undertaken using the conventional ceramic method, which necessitates time-consuming regrinding and repeated firing in order to optimize solid phase reaction. Even following this process the final compound is often compositionally inhomogeneous, with a large grain size distribution, ultimately contributing to low measured critical currents. Various wet-chemical and sol–gel routes [11] (well established in the advanced ceramics field [12]) have also been exploited which facilitate mixing on the atomic level, producing materials of superior quality. Furthermore, a number of papers have apppeared based on an adaptation of a combustion method first introduced by Merzhanov and Borovinkaya [13], and involve combustion of redox mixtures containing the constituent metal nitrates, and a fuel such as urea [14, 15], glycine [15, 16] or more recently maleic hydrazide (3,6 dihydroxypyridazine) [17]. Formally, the term "combustion synthesis" also incorporates routes involving self-sustaining reactions initiated by an external heat source, these are sub-divided into "self-propagating high-temperature synthesis" and "thermal explosion" methods [18]. A specific feature of "wet-chemical" or "combustion" derived oxide precursors in general, is an extremely fine grained microstructure, which would be expected to profoundly influence reactivity and sintering and hence reaction kinetics.

0022–2461

In order to gain an insight into the reaction kinetics and mechanism of $Y_2Cu_2O_5$ formation, we used a combination of conventional quantitative powder X-ray diffraction (XRD) and electron paramagnetic resonance (EPR) spectroscopy to monitor phase formation and to make an assessment of the probable reaction mechanism, with reference to published models. Quantitative XRD data was analysed according to a range of kinetic functions and activation energies calculated. We further exploited this approach to probe the effectiveness of alternative synthetic routes including the use of wet-chemical precursors, combustion synthesis and low-melt accelerants (e.g. $NaNO_3$).

2. Experimental procedure

Samples of $Y_2Cu_2O_5$ were prepared by four routes:

(i) *Ceramic method* Stoichiometric amounts of analytical grade Y_2O_3 and CuO were milled in a cyclohexane slurry, dried and fired in alumina crucibles at 1023, 1048, 1073 and 1098 K for various reaction times.

(ii) *Coprecipitation* 0.1 M sodium hydroxide solution was added slowly with constant stirring to an aqueous mixture of equimolar yttrium (III) and copper (II) nitrates with the pH being maintained at 11.5. The necessity for careful pH control at this stage, has been discussed elsewhere [19]. The blue precipitate was filtered, washed and dried at 433 K for 4 to 6 h, followed by decomposition to the constituent oxides at 823 K for 18 h. The powder was pressed into pellets and sintered at 973, 998 and 1048 K for different reaction times.

(iii) *Combustion synthesis* this uses an aqueous solution containing stoichiometric mixtures of metal nitrates which act as an oxidizer and a fuel – maleic hydrazide. Combustion was carried out at 623 K in a muffle furnace; the resulting voluminous oxide mix was fired according to the conditions under investigation.

(iv) *Ceramic method with accelerant* $NaNO_3$ was added to a stoichiometric mixture of Y_2O_3 and CuO. The sample was initially heated at 873 K followed by pelletizing and firing as in (i).

Scanning electron micrographs of representative samples produced by each method clearly showed the combustion route to yield the smallest grains (1–2 μm) and narrowest size distribution. The hydroxide derived particles were slightly larger, although fairly uniform, whereas the microstructure of samples produced by solid state synthesis revealed a wide range of sizes (typically 2–10 μm) and morphologies.

Powder XRD measurements were carried out using a Phillips PW3020 diffractometer employing CuK_α radiation. Quantitative measurements used TiO_2 (anatase) as an internal standard, facilitating calculation of fractional reaction (α). Constant step size was used for all samples. Peak areas were calculated at reflections $2\theta = 25.180$ (TiO_2) and $2\theta = 31.170$ ($Y_2Cu_2O_5$). Fig. 1 illustrates the components of a typical XRD pattern used to calculate α values.

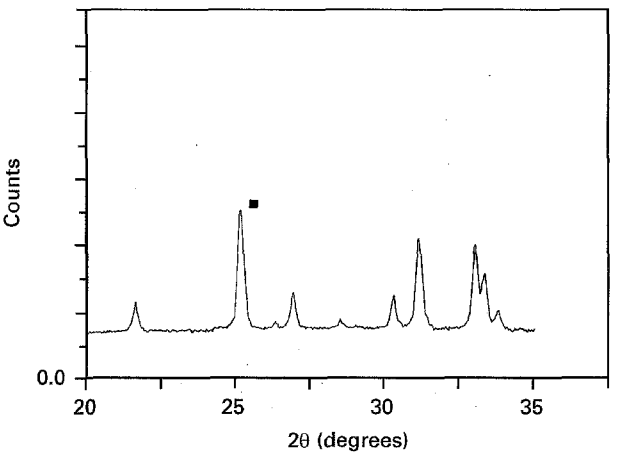

Figure 1 X-ray powder diffraction pattern for a mechanical mix used for quantitative measurement; the TiO_2 reflection is labelled ■.

X-band (9.1 GHz) EPR measurements were obtained using a Bruker ESP-300E spectrometer, with all samples being sealed in Suprasil quartz tubes.

3. Results and discussion

X-band EPR spectra of a sample confirmed as $Y_2Cu_2O_5$ by XRD revealed a broad symmetrical resonance at $g = 2.10$, with a peak-to-peak linewidth of ca. 600 G. This was in accord with previously published data [20]. However, a markedly different spectrum was obtained from a sample reacted at 1023 K for only 15 min (Fig. 2), well defined $^{63/65}Cu$ ($I = 3/2$) electron-nuclear hyperfine coupling is resolved along with a clear g-tensor anisotropy. As the firing temperature is increased, the hyperfine features progressively coalesce until the single line spectrum discussed above, is detected. Loss of metal hyperfine structure is a consequence of decreasing magnetic dilution, and the onset of exchange coupling. We suggest the 1023 K response is characteristic of the initial stages of phase formation, presumably corresponding to initial nucleation at defects or grain boundaries, where individual Cu^{2+} moments are fairly isolated. Following accepted thinking, product formation follows by active interface motion into unchanged reactant, where chemical reaction takes place. We suggest that the EPR response is mirroring this process, and providing a probe of the solid state reaction at the microscopic level, where more conventional methodology XRD, thermogravimetric analysis (TGA), differential scanning calorimetry (DSC) etc. cannot provide information.

Fig. 3 shows isothermal α-time curves for the formation of $Y_2Cu_2O_5$ at a range of temperatures, the data was analysed using standard computer fitting procedures according to the models listed in Table I. XRD traces were compared with a $Y_2Cu_2O_5$ standard, formed by reaction of Y_2O_3 and CuO at 1223 K, for 72 h. This sample showed no trace of starting materials as guaged by XRD, and was used to define the reaction at 100% completion. The best fit obtained was to the Jander equation which is based upon interdiffusion between two flat slabs of reactant, and was

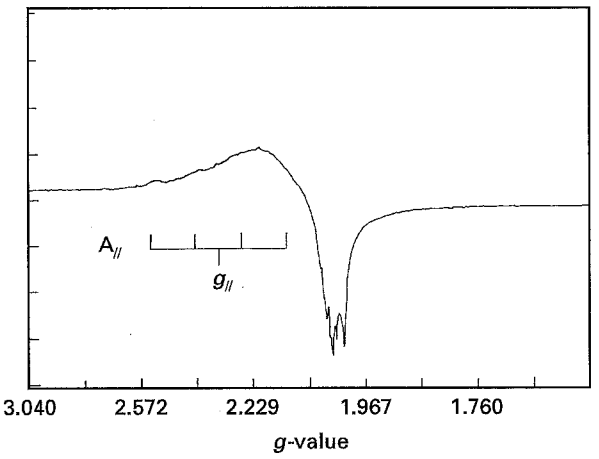

Figure 2 First derivative X-band (9.1 GHz) EPR spectrum, measured at room temperature for a mixture of Y_2O_3 and CuO fired at 1023 K for 15 min.

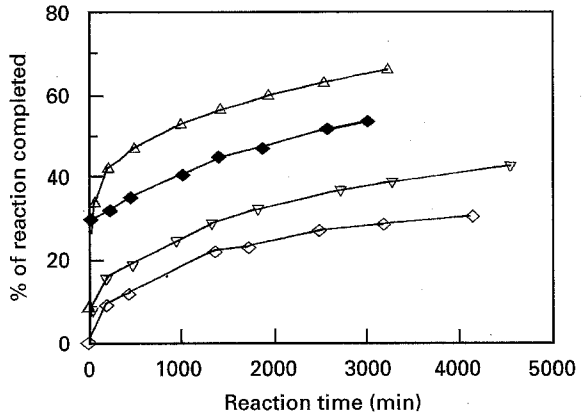

Figure 3 Isothermal plot of percentage of reaction completed for the formation of $Y_2Cu_2O_5$ at a range of temperatures. △ 1098 K; ◆ 1073 K; ▽ 1048 K; ◇ 1023 K.

TABLE I Solid state reaction models, adapted from reference [4]

Reaction models	Kinetic equations
One-dimensional diffusion	$kEt = \alpha^2$
Two-dimensional diffusion	$kEt = \alpha + (1-\alpha)\ln(1-\alpha)$
Jander equation, three-dimensional diffusion	$kEt = [1-(1-\alpha)^{1/3}]^2$
Dunwald–Wagner equation	$kEt = 6/\ln\pi^2(1-\alpha)$
Ginstling–Brounstein equation, three-dimensional diffusion	$kEt = (1-2/3\alpha) - (1-\alpha)^{2/3}$
Two-dimensional phase boundary reaction	$kEt = [1-(1-\alpha)^{1/2}]$
Three-dimensional phase boundary reaction	$kEt = [1-(1-\alpha)^{1/3}]$
First order kinetics	$kEt = [-\ln(1-\alpha)]$
Random nucleation, Avrami equation	$kEt = [-\ln(1-\alpha)]^{1/2}$
Random nucleation, Erofeev equation	$kEt = [-\ln(1-\alpha)]^{1/3}$

kEt = reaction rate constant, t = reaction time (min)
α = fraction of the reaction completed.

the first successful model for solid state reactions, which, (although attracting criticism [21]) has proved applicable in many cases [4]. Indeed, the applicability of this model over a range of firing temperatures is clearly illustrated in Fig. 4. Consideration of the

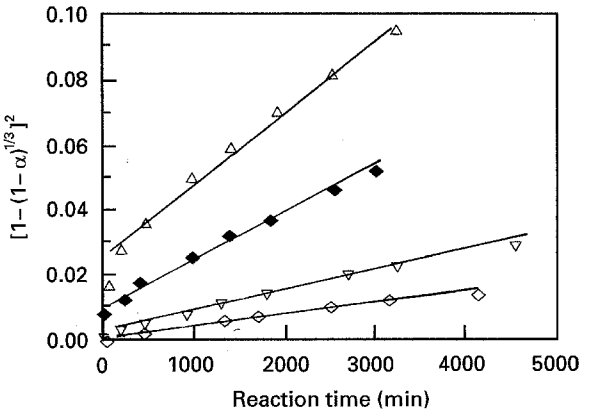

Figure 4 Formation of $Y_2Cu_2O_5$ as a function of temperature, according to the Jander diffusion model. Key as shown in Fig. 3.

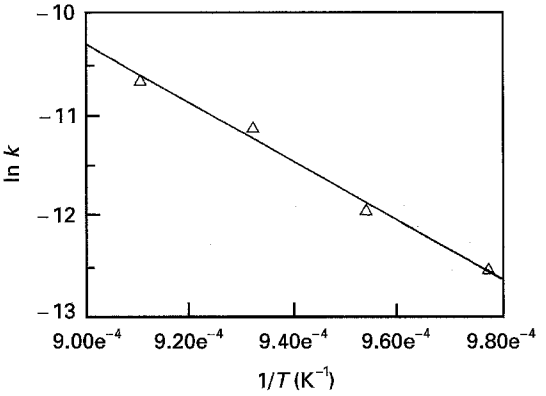

Figure 5 Temperature dependence of rate constants, obtained using the Jander model.

TABLE II Comparison of different synthetic techniques at 1048 K (firing time 1 h)

Synthetic route	α-value
Ceramic	9.375
Precipitation	24.86
Accelerant	29.22
Combustion	67.542

temperature dependence of the rate constants obtained on the basis of the Jander model (Fig. 5) gave a calculated activation energy of 58.2 kcal mol^{-1}. Furthermore, we also point out that the next best fit was with the Ginstling–Brounstein equation, which is again a diffusion based model. This similarity, together with poor fits to models based on phase-boundary reaction, nucleation etc., suggest the reaction of yttrium oxide and copper(II) oxide in the solid state is diffusion controlled.

Quantitative XRD studies were also used to produce a comparison of α values obtained by a range of synthetic methods (Table II). Here we clearly observe significant rate enhancement for the "wet-chemical" methods, particularly the combustion technique, reflecting the small particle size of the reactant, which enables more extensive interfacial reaction and smaller distances for reaction front motion. One notable example where kinetic contraints on synthesis are overcome, is during preparation of superconducting

$YBa_2Cu_4O_8$, where kinetic demands require high oxygen overpressures for conventional ceramic synthesis, but additives such as alkali nitrates or carbonates (where intergranular ionic diffusion is enhanced by the molten additive) [22, 23] or the use of sol–gel methodology [24, 25], facilitate ambient pressure synthesis, in high yield. It is apparent that the preparative approach employed will control the formation mechanism and modify the activation energy. In this regard, studies of the kinetics of reaction via wet chemical and combustion methods (with a natural extension to the superconducting cuprates themselves) are currently underway in our laboratory.

4. Conclusions

The results of this study have shown that the solid-state reaction between Y_2O_3 and CuO is diffusion controlled, with the Jander model providing the most suitable fit to our data. Quantitative powder XRD proved an ideal means of monitoring the progress of reaction, the paramagnetic nature of the product enabled EPR spectroscopy to probe the initiation of the reaction down to product levels far below the XRD detection limits. Certainly, the availability of a convenient means of providing mechanistic information, would reduce the usual "trial and error" approach to obtaining compositionally homogeneous superconductors via solid-state synthesis or other routes, and underpin future developments in synthetic methodology.

References

1. P. GHIGNA, U. ANSELMI-TAMBURINI, G. SPINOLO and G. FLOR, *J. Phys. Chem. Solids* **54** (1993) 107.
2. W. JANDER, *Z. Anorg. Allg. Chem.* **163** (1927) 1.
3. A. M. GINSLING and V. I. BROUNSTEIN, *J. Appl. Chem.* **23** (1950) 1327.
4. A. A. EL-BELLIHI, A. M. ABDEL-BADEI and EL-H. M. DIEFALLAH, *Thermochim. Acta* **165** (1990) 147.
5. W. E. BROWN, D. DOLLIMORE and A. K. GALWEY, in "Chemical kinetics: reactions in the solid state," edited by C. H. Bamford and C. F. H. Tipper (Elsevier, 1980).
6. M. ARJOMAND and D. J. MACHIN, *J. Chem. Soc. Dalton Trans.* (1975) 1061.
7. R. TROC, Z. BUKOWSKI, R. HORYN and J. KLAMUT, *Phys. Lett.* **125** (1987) 222.
8. C. CARBONI and D. CIOMARTAN, *J. Magn. Magn. Mater.* **104–107** (1992) 939.
9. R. HORYN, J. KLAMUT, M. WOLCYRZ, A. WOJAKOWSKI and A. J. ZALESKI, *Ibid.* **140–144** (1995) 1575.
10. Q. SU, X. CAO and H. WANG, *J. Mater. Chem.* **4** (1994) 417.
11. Y. G. METLIN and Y. D. TRETYAKOV, *Ibid.* **4** (1994) 1659.
12. D. SEGAL "Chemical synthesis of advanced ceramic materials" (Cambridge University Press, Cambridge, 1989).
13. A. G. MERZHANOV and I. P. BOROVINSKAYA, *Dolk. Acad. Nauk.* **204** (1972) 366.
14. R. MAHESH, A. VIKRAM, O. PRAKASH and C. N. R. RAO, *Supercond. Sci. Technol.* **5** (1992) 174.
15. H. VARMA, K. G. WARRIER and A. D. DAMODARAN, *J. Amer. Ceram. Soc.* **73** (1990) 3103.
16. L. R. PEDERSON, G. D. MAUPIN, W. J. WEBER, D. J. McREADY and R. W. STEPHENS, *Mater. Lett.* **10** (1991) 437.
17. R. GOPI CHANDRAN and K. C. PATIL, *Mater. Res. Bull.* **27** (1992) 14.
18. J. P. LEBRAT and ARVIND VARMA, *Combust. Sci and Technol.* **88** (1992) 177.
19. M. J. PARKER and R. JANES, *J. Mater. Sci.* **28** (1993) 4515.
20. R. JONES, R. JANES, R. ARMSTRONG, N. C. PYPER, P. P. EDWARDS, D. J. KEEBLE and M.R. HARRISON, *J. Chem. Soc. Faraday Trans.* **86** (1990) 675.
21. R. E. CARTER, *J. Chem. Phys.* **34** (1961) 2010.
22. R. J. CAVA, J. J. KRAJEWSKI, W. F. PECK, B. BATLOGG, L. W. RUPP, R. M. FLEMING, A. C. W. P. JAMES and P. MARSH, *Nature* **338** (1989) 328.
23. D. M. POOKE, R. G. BUCKLEY, M. R. PRESLAND, and J. L. TALLON, *Phys. Rev.* **B41** (1990) 6616.
24. S. KORIYAMA, T. IKEMACHI, T. KAWANO, H. YAMAUCHI and S. TANAKA, *Physica C* **185–189** (1991) 519.
25. R. S. LIU, R. JANES, M. J. BENNETT and P. P. EDWARDS, *Appl. Phys. Lett.* **57** (1990) 920.

Received 8 December 1995
and accepted 15 January 1996